Proceedings of ISFOG 2025
5TH INTERNATIONAL SYMPOSIUM ON
FRONTIERS IN OFFSHORE GEOTECHNICS
Nantes, France | June 9-13 2025

ISBN 978-2-85782-758-0

A framework for analysis of pile run

T. Vergote*, G. Haine, S. Raymackers
DEME Offshore, Zwijndrecht, Belgium

A. Burgraeve
Cathie Group, Brussels, Belgium

**Vergote.Thomas@deme-group.com*

ABSTRACT: Pile run prediction is of increasing importance in offshore wind as it is a threat to the integrity of the foundation, the installation equipment and the support vessel. There is a need for improved methodology for assessing the risk of triggering a pile run and the distance over which the pile might be running before the soil resistance is sufficient to stop it. The current approach, typically a factorization of the soil resistance to driving, has shown unable to predict accurately the extension of a pile run when triggered and could be unconservative in soils with a high sensitivity to the loading rate. The result of a literature review on rate-dependency behaviour of soils is presented after which a framework is developed for analysis of a "rate dependent" soil resistance, the framework is then applied to the case of a large pile run. Conclusions are drawn on the applicability of the proposed framework and additional research needed for further development.

Keywords: Pile run; prediction; critical state; rate-dependence

1 INTRODUCTION

Offshore foundations of wind turbines are commonly founded on piles, consisting of large steel pipes in the range of 3 to 12m diameter, which will be inserted into the seafloor by means of impact hammer.

When during this process an imbalance exists between the load and the soil resistance, penetration will occur. If this happens during pile stabbing, hammer stabbing or the driving process, it is called a pile run. If the imbalance becomes large and the pile is unrestrained, it will result in an uncontrolled sudden penetration or "free-fall".

Three phases can be distinguished in a pile run: initiation, acceleration, deceleration. Initiation might occur when reaching a weaker layer (punch-through), by soil strength degradation (sensitivity or pore pressure build-up), or as a consequence of a hammer blow or sudden increase of load. When the pile is in "free-fall", the soil resistance can be further affected during the acceleration and deceleration phases by the pile velocity. Deceleration might happen progressively as the result of a friction build-up along the shaft or abruptly if the pile enters a layer which offers large end bearing.

For predicting initiation and final penetration depth of the pile during a run, which is of primary importance for a contractor to foresee correct mitigation measures, accurate methods are required. Experiments on the penetration of projectiles in soft soils led to the development of a prediction method of the penetration depth based on the motion equation (True, 1975). It included an empirical approach to account for strain-rate effects. (Sun et al, 2022) proposed an analytical method to calculate the depth range and the profile of pile velocity. It is based on the second law of Newton, using API with a dependency of the shear strength on the strain rate by a power function, or a CPT-based method with friction fatigue to calculate the soil resistance. The method is applied on a case study of the installation of 158m long piles with a diameter of 2.743m in the South China Sea, during which multiple pile runs occurred.

An approach was recently developed by (Thijssen and Roelen, 2024) using an energy conservation model to predict the extent and the velocity of a pile run. The soil resistance is calculated with a CPT-based method. The risk for liquefaction and the sensitivity to strain-rate effects are evaluated.

The present paper suggests a novel framework modelling a pile run using an energy conservation equation and integrating the rate effect on the soil resistance by means of a backbone curve, describing the change in soil resistance between drained to fully undrained conditions. To define the limits (drained/undrained) of the backbone curve, a critical state framework is adopted, used to derive the undrained resistance of the soil from CPT results.

2 MODEL SET-UP

2.1 Pile run and kinetic energy dissipation

A pile run occurs if there is a disequilibrium between the soil resistance acting on the pile, F_{soil} and the total applied weight W, which may consist of the pile W_{pile} or the combined weight of hammer and pile $W_{pile} + W_{hammer}$, possibly reduced by a lifting force of the crane F_{crane} or uplift air pressure F_{air}. These factors combined constitute the pile run force F_{run}. The onset of pile run happens if:

$$W_{pile} + W_{hammer} - F_{crane} - F_{air} = F_{run} > F_{soil} \quad (1)$$

Once the pile starts to accelerate, kinetic energy E_k is built up. The total amount of work delivered due to the displacement of pile is caused by the net resistance $(F_{soil} - F_{run})$. This could both accumulate (accelerate) kinetic energy or dissipate the energy depending on the equilibrium of forces.

At any depth, the kinetic energy of the pile can be expressed as:

$$E_k(z) = E_k(z_0) - \int_{z_0}^{z} (F_{soil} - F_{run})\, dz \quad (2)$$

with z_0 the depth at which the pile run starts. Considering $E_k = \frac{1}{2} m \cdot v^2$, the velocity of the pile is given as:

$$v(z) = \sqrt{\frac{2\left(E_k(z_0) - \int_{z_0}^{z}(F_{soil} - F_{run})dz\right)}{m}} \quad (3)$$

This can be calculated by discretization of Δz using a finite difference approximation.

A CPT-based approach is used to calculate F_{soil}. As a basis, the expression of (Alm and Hamre, 2001) is used. This method includes the end bearing and shaft resistance of the pile, with consideration of friction degradation as the pile moves further through the soil. Thanks to the incorporation of the kinetic energy, it is possible to model a pile that punches through a stronger soil if the velocity is sufficiently high. As such it improves on the prediction of the pile run response.

2.2 Rate effects

The soil resistance during pile installation is typically derived from a CPT, which is executed at 2cm/s. Loading rate effect on q_c have been investigated by centrifuge testing (Chung et al., 2006; Danziger and Lunne, 2012; DeJong and Randolph, 2012; Price et al., 2019) simulating a CPT testing in kaolin clay or silty soils. Field CPTUs tests at various rates in a saturated clayey silt were reported by (Martínez et al., 2016) and showed a good correlation with the curve developed by (DeJong and Randolph, 2012).

By varying the CPT penetration rate, the resistance to different shearing condition (drained, partially drained, undrained) is tested. The studies result in a backbone curve, which describes the relation between the normalised cone resistance $Q = (q_t - \sigma_{v0})/\sigma'_{v0}$ and the normalised velocity $V = (v \cdot d)/c_v$, with q_t the corrected cone resistance, σ_{v0} the total vertical stress, σ'_{v0} the effective vertical stress, v the velocity (of pile or cone), d the (equivalent) diameter and c_v the coefficient of consolidation.

The diameter for a CPT is typically 35.7mm (for 10cm^2 cones). For a large open-ended pile, which will be coring during installation, the equivalent diameter can be taken as the pile toe thickness. In Table 1 different normalised velocities are derived for comparison.

The rate-effects can be now be quantified using a relation between the normalised cone resistance Q and the normalized velocity V as (DeJong and Randolph, 2012):

$$\frac{Q}{Q_{ud,ref}} = 1 + \frac{Q_{dr}/Q_{ud} - 1}{1 + (V/V_{50})^c} \quad (4)$$

with Q_{ud} and Q_{dr} the normalised cone penetration under undrained and drained conditions respectively, V_{50} the normalised velocity corresponding to half of the excess pore pressure mobilization and c the maximum rate of change. (DeJong and Randolph, 2012) suggest values of $V_{50} = 3$ and $c = 1$.

The ratio Q_{dr}/Q_{ud} (eq. 4) defines the total change in resistance and is a critical value to define. It is to be noted that the viscous effect during undrained penetration, which may lead to an increase in Q beyond Q_{ud}, is not explicitly considered here.

Table 1. Normalised velocity V for c_v= 0.03 m²/s (sand)

	v [m/s]	d [m]	V [-]
CPT	0.02	0.0357	0.02
Pile stabbing	0.02	0.1	0.06
Pile driving during a blow (0.01m/10ms)	1	0.1	3.15
Pile run low speed	2	0.1	6.31
Pile run high speed	10	0.1	31.54

2.3 Application of rate effects on the pile resistance

The CPT-based soil resistance model provides a measure for the end-bearing $q_b(d_e)$ and unit shaft friction $f_{s,pile}(z, d_e)$ with d_e the embedded depth of the pile and z the depth. The cone resistance can be converted to fully undrained conditions, $q_{b,ud,ref}$ and $f_{s,ud,ref}$ and finally to end-bearing and sleeve friction of the pile. This is done with the assumption that q_b and f_s can be scaled linearly with Q:

$$q_{b,v=v_{pile}}(d_e) = q_b(d_e) \cdot \frac{Q_{v=v_{pile}}(\mathrm{d_e})}{Q_{v=v_{cpt}}(\mathrm{d_e})} \tag{5}$$

$$f_{s,v=v_{pile}}(z, d_e) = f_s(z, d_e) \cdot \frac{Q_{v=v_{pile}}(\mathrm{z})}{Q_{v=v_{cpt}}(\mathrm{z})} \tag{6}$$

The ratio Q/Q_{ud} is both velocity and depth dependent because the coefficient of consolidation c_v varies. For clay layers where $Q_{v=v_{cpt}}$ is already undrained, faster rates will not further affect the ratio (excl. viscous effects) while for sand layers with higher c_v value the effect may be very significant.

Once the end bearing and unit shaft friction are factored by the rate-effect, they can be integrated to provide the full resistance:

$$F_{soil}(v, d_e) = q_{b,v}(d_e)A_{annulus} + \sum_0^{d_e}[f_{s,v}(d_e, z)\Delta A_{shaft}\Delta z] \tag{7}$$

With $A_{annulus}$ the area of the annulus of the pile and ΔA_{shaft} the shaft area per meter at a given depth.

The model has been set up to calculate the rate effect at every time step and apply it over the embedded length of the pile in accordance to the c_v values.

2.4 Undrained cone resistance and the state parameter

To consider the rate-effects properly, an objective estimation of the ratio Q_{dr}/Q_{ud} is required. This ratio could be significantly larger than 1 or smaller than 1 depending on the contractive or dilative state of the soil, respectively. While most research on rate-effects in CPTs has been done on contractive, fine-grained soils, some experimental work showcases dilative behaviour with an increase of the cone resistance at higher rates for silts and sands, (Danziger and Lunne, 2012; DeJong et al., 2013; Price et al., 2019; Schneider et al., 2007).

A framework for sand is proposed by (White et al., 2018) which relies on the relative density of the soil, D_r and the relative dilatancy I_R (Bolton, 1986).

The undrained shear strength s_u can be calculated within the critical state framework as:

$$s_u = \frac{1}{2}p_f'\left(\frac{6\sin\phi_{cv}'}{3-\sin\phi_{cv}'}\right) = \frac{1}{2}Mp_f' \tag{8}$$

With ϕ_{cv}' the friction angle at constant volume, M the slope of the critical state line and with $p_f{}'$ the stress at undrained failure. Finally, the undrained net cone resistance $q_{net,ud}$ is given as:

$$q_{net,ud} = N_{kt}s_u \tag{9}$$

The bearing factor N_{kt} is selected as 12 in (White et al., 2018), in line with fine-grained soils. Due to a lack of experimental results for sand, this remains an uncertain factor in the approach.

The undrained cone resistance can be compared to the drained cone resistance measured in sands to get Q_{dr}/Q_{ud}. The ratio is the applied in backbone curves like eq. (4). The approach of (White et al., 2018) results in increases or reductions in cone resistance depending on the relative density D_r correlated from the CPT results.

The disadvantage of this approach is that it can only be applied to clean sand and relies on a selected method to derive the relative density. An alternative approach is considered using the state parameter ψ which gives a more direct indication of dilative versus contractive responses. Within a simple critical state framework, (Jefferies and Been, 2016), the state parameter provides a direct indication of the undrained shear strength considering the effective stress $p_f{}'$:

$$p_f' = p_0' \exp\left(-\frac{\psi}{\lambda}\right) \tag{10}$$

With p_0' the initial effective stress and λ the compression index. The undrained shear strength can then be calculated using eq. (8). While this approach is promising and has a sound theoretical basis, the state parameter ψ still relies on an uncertain CPT correlation. Two well-established correlations were considered, (Jefferies and Been, 2016; Robertson, 2010) for sandy soils, respectively:

$$\psi = -\frac{\ln([Q_p(1-B_q)+1]/\bar{k})}{\bar{m}} \tag{11}$$

$$\psi = 0.56 - 0.33\log Q_{tn,cs} \tag{12}$$

With $\overline{m}$ and $\overline{k}$ empirical factors which are correlated to λ, Q_p the normalized cone resistance by mean effective stress and $Q_{tn,cs}$ the stress-normalized cone resistance and B_q the normalised pore pressure. The compression index λ can be correlated to I_c or F_r (Jefferies and Been, 2016). The undrained shear strength of the sand can now be derived from eq. (8). Alternatively, the expression proposed by (Robertson, 2022, 2010) can be used:

$$\frac{s_u}{\sigma_{v0}'} = 0.0007\exp\left(0.084Q_{tn,cs}\right) + \frac{0.3}{Q_{tn,cs}} \qquad (13)$$

This expression only applies for $20 < Q_{tn,cs} < 80$ considering liquefaction and may represent a lower bound of the real resistance during a pile run.

Ayala et al. (2023) presents calibrated factors $\overline{m}$ and $\overline{k}$ for both drained Q_{dr} and undrained Q_{ud} shearing , $\overline{m}_{dr} = 5.73$, $\overline{k}_{dr} = 45.11$, $\overline{m}_{ud} = 20.48$, $\overline{k}_{ud} = 17.65$ for platinum tailings. With these factors, Q_{ud}/Q_{dr} can be calculated directly for a given ψ.

To evaluate the relations, a sensitivity study was done on the different components of the backbone curve. Figure 1 compares the state parameter as calculated by eq. 11 and 12 for given I_c, B_q and correlated λ. It can be observed that this varies significantly, especially on the contractive side. This variation also leads to significant variation in the undrained shear strength estimates given in Figure 2.

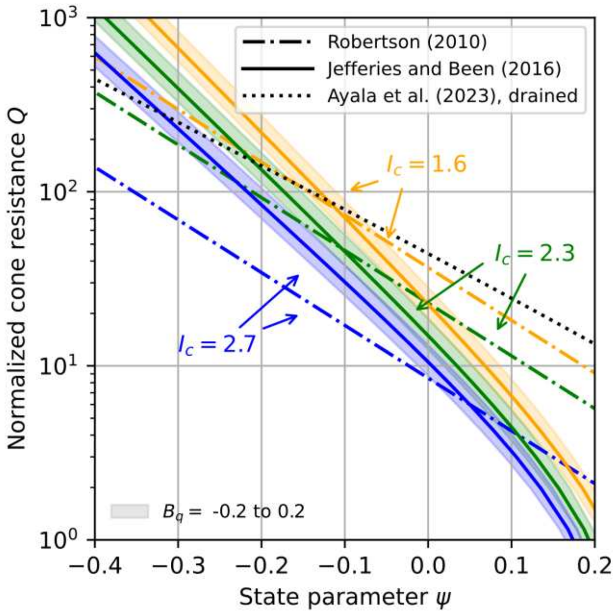

Figure 1. Sensitivity of state parameter correlations of (Jefferies and Been, 2016; Robertson, 2010)

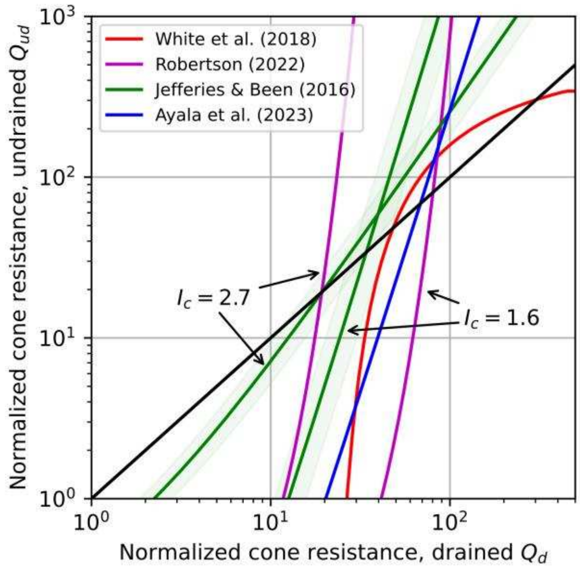

Figure 2. Sensitivity of strength reduction for different methods ($\sigma_v' = 200kPa, K_0 = 1$)

2.5 Cavitation during dilation

In case of dense (sandy) soils, the undrained shear strength increases significantly due to negative excess pore pressures u_e depending on the (negative) state parameter ψ. The pore pressures lead to an increase in p_f' which finally lead to large undrained Q_{ud}. If the excess pore pressures drop below the total absolute stress (including water and air pressure), cavitation would occur. At that point, pore pressures cannot go down further, (Ibsen, 1995; Mcmanus and Davis, 1997). This limits the increase in the effective stress to a value that can be expressed as:

$$p'_{max} = p_0 + u_{00} + p_a \qquad (14)$$

With p_0 the total pressure (measured from seabed), u_{00} the water pressure at the seabed and p_a the air pressure. In case of $K_0 = 1, p_0 = \sigma_v$. Note that the cavitation limit depends on the penetrated depth, but also the water depth. This cavitation limit can be applied in every model, by calculating a maximum undrained shear strength, $s_{u,max}$ using eq. 8.

To illustrate the effect of this cavitation limit, the backbone curves as reported by (White et al., 2018) for z=2m, are replicated and backbone curves considering cavitation (Figure 3) are added. Contractive soil leads to a reduction in q_c during increased velocity, while dilative soils may exhibit an increase or reduction in q_c, if affected by cavitation.

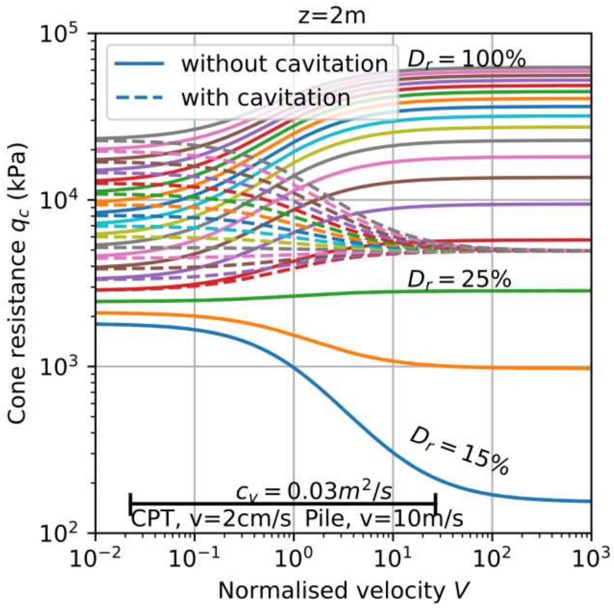

Figure 3. Replication of backbone curves calculated with the method of (White et al., 2018), the effect of cavitation is added for a water depth of 40m and 2m penetration.

3 MODEL APPLICATION

3.1 Pile run case

The modelling approach has been applied to a real pile run case to test its applicability. The case consists of a free-fall of a single pile from 2m into the seabed up to 59m. The pile had an initial velocity of 0m/s. Soils consisted of a mix of silty sands, silts and more clayey layers. The model was made with $N_{kt} = 12$, $c_v = 0.03\ m^2/s$ (sand) and $6.34\ 10^{-8}\ m^2/s$ for clay. A video footage of the pile run allowed to digitize the penetration in function of time. A polynomial function was fitted to the penetration profile and used to derive the velocity profile.

3.2 Inferred soil resistance from velocity profile

Based on the measured velocity of the pile, the real kinetic energy can be calculated. This can in turn be used to infer the soil resistance applied on the pile as:

$$F_{soil} = \frac{dE_k}{dz} + F_{run} \tag{15}$$

This can be approximated with finite differences to provide a profile over depth, as included in Figure 4.

3.3 Results

The pile run velocity is predicted for several modelling approaches (Figure 4). The soil resistance without rate effects, F_{soil} exceeds the downward force F_{run} at 17m. The basic prediction without any rate effects, considering only the dissipation of kinetic energy leads to a predicted pile run of about 31m, considerably beyond the point where $F_{run} < F_{soil}$ but much less than the observed pile run of 59m.

Rate effects change the picture considerably: at the top the soil tends to be dilative ($\psi < -0.05$) for most models, and at greater depth the soil is clearly contractive leading to significantly lower Q_{ud} and further pile run. However, due to larger Q_{ud} at the top, the pile run is stopped in its track as the resistance increases with pile acceleration. After consideration of cavitation, the predicted acceleration tends to be more in line with the recorded pile run.

An attempt is made to calibrate the critical state-based model (eq. 8, 9 and 11) by adjusting $\bar{m}, \bar{k}$ and λ. This results in the given "fit", which replicates the overall pile run, albeit at a maximum velocity which exceeds the observations.

4 CONCLUSIONS & FURTHER WORK

When a pile is in free fall the kinetic energy can cause the pile to run deeper than expected, further on the pile velocity can induce the soil to behave more undrained than during a CPT. A framework is proposed to analyse pile velocity in function of the rate-dependent soil resistance. The rate dependence is calculated using backbone curves that depend on the state parameter, which is used to quantify the undrained shear strength with critical state theory. In addition, the effects of cavitation have been included, which sets a limit to the undrained shear strength.

The framework is applied to a test case using Alm & Hamre (2001) for the initial soil resistance (at CPT penetration velocity). The case demonstrates that kinetic energy alone is insufficient to predict the full pile run, while rate effects improve the prediction. By tuning the correlation of the state parameter, it is possible to calibrate the model to the specific case.

Further calibration will be required though to establish a unique most reliable method for pile runs in different soils.

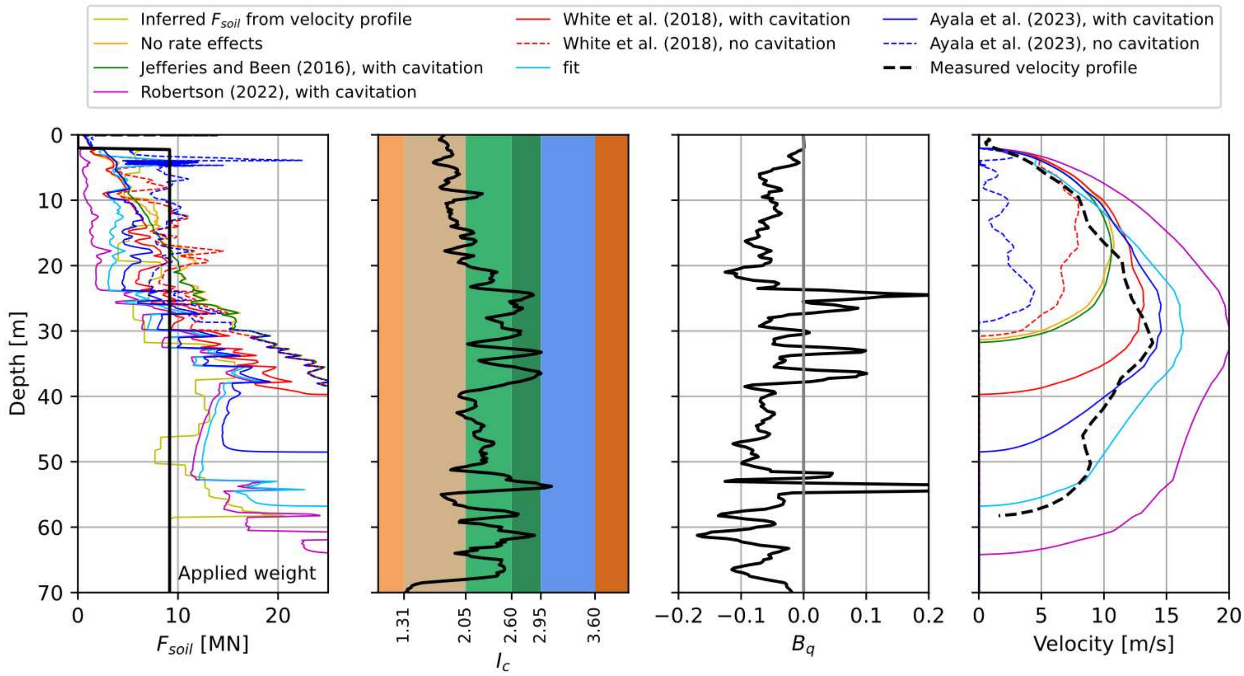

Figure 4. Case study of a large pile run with measured and predicted velocity profile

We hope to emphasise the need for good site investigation campaigns, to derive the parameters needed for the simulations. Especially permeability tests could be of added value to evaluate the likelihood of undrained behaviour. We hope to inspire other (academic) researchers to document more cases.

Further research is needed to evaluate adequate cut-off levels due to cavitation and more generally backbone curves for sand on the dry side of critical.

AUTHOR CONTRIBUTION STATEMENT

Thomas Vergote: Formal Analysis, Writing - Original draft, Software, Visualization. **Alain Burgraeve**: Data curation, Conceptualization, Writing - Original draft. **Geoffroy Haine**: Reviewing and Editing. **Sylvie Raymackers**: Writing, reviewing and Editing, Supervision.

REFERENCES

Alm, T., Hamre, L. (2001). Soil model for pile driveability predictions based on CPT interpretations, In: *International Conference on Soil Mechanics and Geotechnical Engineering Proceedings,* Istanbul, Türkiye, pp. 1297–1302.

Ayala, J., Fourie, A., Reid, D. (2023). A Unified Approach for the Analysis of CPT Partial Drainage Effects within a Critical State Soil Mechanics Framework in Mine Tailings. *J. Geotech. Geoenviron. Eng.* Volume 149 Issue 6, https://doi.org/10.1061/JGGEFK.GTENG-10915

Bolton, M.D. (1986). The strength and dilatancy of sands. *Géotechnique,* Volume 36, pp. 65–78. https://doi.org/10.1680/geot.1986.36.1.65

Chung, S., Randolph, M.F., Schneider, J. (2006) Effect of penetration rate on penetrometer resistance in clay. *Journal of Geotechnical and Geoenvironmental Engineering,* Volume 132 Issue 9, pp. 1188–1196. https://doi.org/10.1061/(ASCE)1090-0241(2006)132:9(1188)

Danziger, F.A.B., Lunne, T. (2012). Rate Effect on Cone Penetration Test in Sand. *Geotechnical Engineering Journal of the SEAGS & AGSSEA,* Volume 43 No. 4, pp. 72–81.

DeJong, J.T., Jaeger, R.A., Boulanger, R.W., Randolph, M.F., Wahl, D.A.J. (2013). Variable penetration rate cone testing for characterization of intermediate soils, In: *Geotechnical and Geophysical Site Characterization 4*. Taylor & Francis Group, Porto de Galinhas, Brazil, pp. 25-42

DeJong, J.T., Randolph, M. (2012). Influence of Partial Consolidation during Cone Penetration on Estimated Soil Behavior Type and Pore Pressure Dissipation Measurements. *J. Geot. Geoenviron Eng.,* Volume 138 No. 7, pp. 777–788. https://doi.org/10.1061/(ASCE)GT.1943-5606.0000646

Ibsen, L.B. (1995). The Static and Dynamic Strength of Sand, In: *Proc. 11th European Conference on*

Soil Mechanics and Foundation Engineering. Copenhagen, Denmark.

Jefferies, M., Been, K. (2016). *Soil Liquefaction - A Critical State Approach, Second Edition*. ed, Applied Geotechnics Series. CRC Press, Taylor & Francis Group. https://doi.org/10.1201/b19114

Martínez, M.F.G., Tonni, L., Gottardi, G., Rocchi, I. (2016). Influence of penetration rate on CPTU measurements in saturated silty soils, In: *Geotechnical and Geophysical Site Characterisation 5*. Sydney, Australia, pp. 473-478.

Mcmanus, K.J., Davis, R.O. (1997). Dilation-induced pore fluid cavitation in sands. *Géotechnique*, Volume 47, pp. 173–177. https://doi.org/10.1680/geot.1997.47.1.173

Price, A.B., Boulanger, R.W., DeJong, J.T. (2019). Centrifuge Modeling of Variable-Rate Cone Penetration in Low-Plasticity Silts. *J. Geot. Geoenviron Eng.,* Volume 145 Issue 11. https://doi.org/10.1061/(asce)gt.1943-5606.0002145

Robertson, P.K. (2022). Evaluation of flow liquefaction and liquefied strength using the cone penetration test: an update. *Can. Geotech. J.,* Volume 59 No. 4, pp. 620–624. https://doi.org/10.1139/cgj-2020-0657

Robertson, P.K. (2010). Evaluation of Flow Liquefaction and Liquefied Strength Using the Cone Penetration Test. *J. Geotech. Geoenviron. Eng.*, Volume 136 No. 6, pp. 842–853. https://doi.org/10.1061/(ASCE)GT.1943-5606.0000286

Schneider, J., Lehane, B., Schnaid, F. (2007). Velocity effects on Piezocone measurements in normally and over consolidated clays. *International Journal of Physical Modelling in Geotechnics*, Volume 7 Issue 2, pp. 23–34. https://doi.org/10.1680/ijpmg.2007.070202

Sun, L., Shi, J., Zhang, Y., Feng, X., Tian, Y. and Wang, R. (2022) Analytical method for predicting pile running during driving, *Applied Ocean Research*, Volume 125. https://doi.org/10.1016/j.apor.2022.103234

Thijssen, R., Roelen, S. (2024). Prediction of Pile Run During Pile Driving - Analytical Model and Field Observations, In: *Offshore Technology Conference, OTC,* Houston, Texas, USA, OTC-35471-MS. https://doi.org/10.4043/35471-MS

True, D.G. (1975), Penetration of Projectiles into Seafloor Soils, Civil Engineering Laboratory (Navy), Port Hueneme, California, USA

White, D.J., O'Loughlin, C.D., Stark, N., Chow, S.H., (2018). Free fall penetrometer tests in sand: determining the equivalent static resistance, In: *Cone Penetration Testing 2018*, CRC Press, London, United Kingdom, pp. 695-701.